

PERSPECTIVE

Optical Coherence Tomography Angiography Signs of Vascular *Abnormalization* With Antiangiogenic Therapy for Choroidal Neovascularization



RICHARD F. SPAIDE

- **PURPOSE:** To investigate the vascular appearance of choroidal neovascularization (CNV) treated with recurrent intravitreal anti-vascular endothelial growth factor (VEGF) injections, which have been proposed to cause transient vascular normalization along with decreased vascularity and leakage.
- **DESIGN:** Retrospective case series with perspective on the topic.
- **METHODS:** Patients with treated CNV secondary to age-related macular degeneration from a community-based retinal referral practice were evaluated with optical coherence tomography angiography employing split-spectrum amplitude decorrelation. The choroidal neovascular morphology of the 17 eyes of 14 consecutive patients was described.
- **RESULTS:** The mean age of the patients, 8 men and 6 women, was 78.4 (standard deviation \pm 9.3) years. The mean greatest linear dimension of the lesion was 3600 μ m. The mean number of anti-VEGF injections was 47 (\pm 21). The vascular diameter of the vessels in the CNV appeared large even in small lesions, with feeder vessels approaching the size of the major arcade vessels of the retina. The vessels had few branch points and many vascular anastomotic connections among larger vessels. There was a paucity of capillaries visualized within the lesions.
- **CONCLUSIONS:** The findings of this study do not support the hypothesis of vascular normalization in eyes receiving recurrent periodic antiangiogenic treatment. The observed “abnormalization” of the vessels may be explained by periodic pruning of angiogenic vascular sprouts by VEGF withdrawal in the face of unimpeded arteriogenesis. As the eye is a readily accessible VEGF laboratory, features expressed therein may also apply to

neovascularization elsewhere in the body, such as in tumors. (Am J Ophthalmol 2015;160(1):6–16. © 2015 by Elsevier Inc. All rights reserved.)

ORGANISMS EMPLOY SEVERAL DIFFERENT STRATEGIES to grow and maintain blood vessels to deliver proper amounts of oxygen and metabolites to tissue, as well as to remove wastes produced by metabolism. The mechanisms used to create new vascular networks include vasculogenesis, a term used to denote the formation of vessels de novo from endothelial precursor cells; angiogenesis, the formation of new capillaries from preexisting vessels; and arteriogenesis, which is the expansion of previously formed channels into larger vessels. While the modes of vessel formation and development may seem to be specific names given to a seamless gradation of vessel proliferation, there are significant differences in how this occurs and what causes each of these changes. Therefore there are potential features that could be targeted in preventing progression in diseases in which vessel growth is a significant feature, such as neovascular age-related macular degeneration (AMD).

A principal configuration in which neovascular AMD appears is as a fibrovascular pigment epithelial detachment (PED).¹ The newly growing vessels elevate the retinal pigment epithelium (RPE) by their physical presence, exudation, bleeding, and any associated fibrotic proliferation. Fluid leaks from the vessels and can accumulate either below or above the RPE monolayer or within the retina.² Intravitreal treatment with anti-vascular endothelial growth factor (VEGF) agents may cause a reduction of the fluid leakage, but it is common to see persistence of fluid despite treatment. Patients require monthly treatment, or at least frequent follow-up and recurrent treatment, to optimize visual outcome. Signs of exudation from neovascularization quickly return even though anti-VEGF agents decrease both angiogenesis and vascular leakage. The appearance and physiology of vessels in treated fibrovascular PEDs is largely unknown, but may have bearing on the need for chronic, frequent treatment. Introduction of

Accepted for publication Apr 7, 2015.

From Vitreous Retina, Macula Consultants of New York, New York, New York.

Inquiries to Richard F. Spaide, Vitreous Retina, Macula Consultants of New York, 460 Park Ave, 5th Floor, New York, NY 10022; e-mail: rickspaide@gmail.com

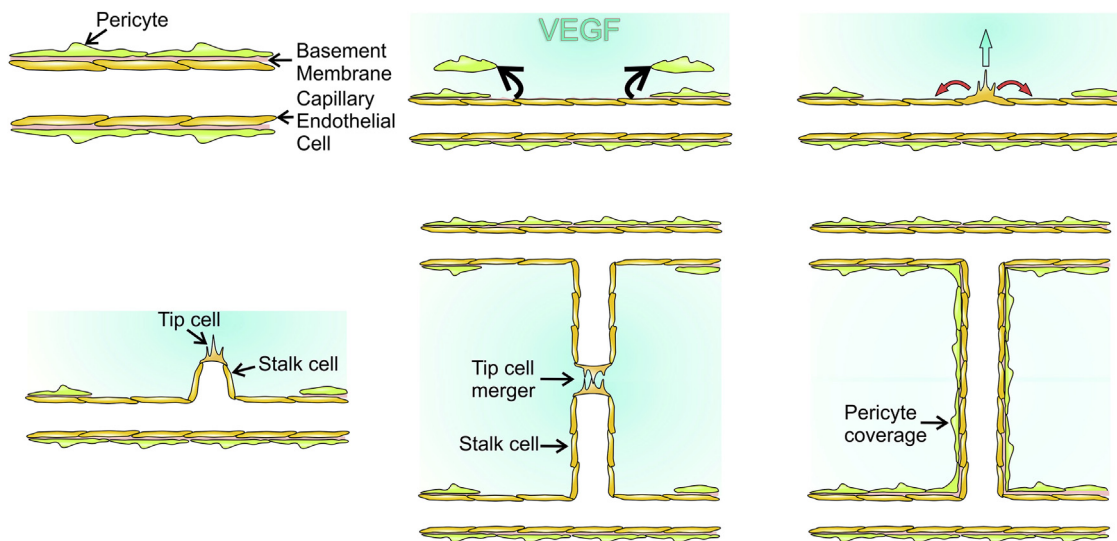


FIGURE 1. The stages of angiogenesis. (Top left) Diagrammatic representation of the main components of a capillary, the endothelial cells, pericytes, and basement membrane. (Top middle) Under the action of vascular endothelial growth factor (VEGF) the pericytes detach from the basement membrane, matrix metalloproteinases are released and break down the basement membrane, and (Top right) some cells become “tip” cells. These cells release inhibitors (red arrows) to prevent the surrounding endothelial cells from differentiating into tip cells. (Lower left) The tip cells develop filopodia that extend outward. The tip cell advances along the VEGF gradient and the trailing endothelial cells, called stalk cells, proliferate to form the nascent capillary stalk. (Bottom middle) The tip cells migrate and eventually merge as an initiating event in vascular anastomosis. (Bottom right) The vascular tube forms, flow commences, the basement membrane is made, and pericyte coverage is elicited. These responses are generic through the body and not ocular-specific.

the basic concepts of vascular development and morphology in health and disease will be presented prior to shifting to the findings specific to treated choroidal neovascularization (CNV).

ANGIOGENESIS

THE SPROUTING OF VASCULAR ENDOTHELIAL CELLS TO FORM new vessels from preexisting vessels is chiefly stimulated by VEGF, along with a host of minor players (Figure 1).^{3,4} Vascular endothelial cells and their mural cells have a common basement membrane. Under the influence of proangiogenic cytokines the mural cells detach and matrix metalloproteinases are released to break down the basement membrane.^{5,6} Interactions between Notch activity and the endothelial cells help in the selection of some of the endothelial cells to become tip cells, which lead the neovascular vanguard. The tip cells laterally inhibit neighboring endothelial cells from being tip cells; instead, they become what are known as stalk cells. The tip cells migrate in the direction of the VEGF gradient and help lead the proliferating stalk cells. Tip cell fusion initiates anastomosis with neighboring vascular outgrowths as mediated by vascular endothelial cadherin, also called VE-cadherin. The stalk cells establish a lumen and create a basement membrane, and perfusion begins. Vessel maturation is marked by reduced proliferation of endothelial cells, pericyte

recruitment, pericyte maturation, and increased formation of cell junctions. Vessel maturation depends on a number of factors, a notable one being transforming growth factor (TGF) β , which participates in mural cell proliferation and migration, as well as in deposition of extracellular matrix. Platelet-derived growth factor (PDGF) participates in the recruitment, migration, and proliferation of both pericytes and smooth muscle cells, as does the bioactive lipid sphingosine-1-phosphate. Angiopoietin-1, produced by pericytes, activates the endothelial receptor tyrosine kinase with immunoglobulin-like and EGF-like domains 1, more conveniently known as TIE1, which helps stabilize vessels, promotes pericyte adhesion, and affects vascular tight junctions.³⁻⁶

Angiogenesis is a continued process that is elicited as needed and continues in a progressive manner until the stimulus for vessel proliferation is abated. The process of angiogenesis can be modulated or blunted by pharmacologic intervention, but the underlying stimulus may not necessarily be affected. Angiogenesis is highly VEGF dependent and targeting VEGF has been a strategy in the treatment of many diseases involving the eye, as well as diseases outside of the eye, including cancer.

ARTERIOGENESIS

THE DILATION OF VESSELS IN RESPONSE TO HIGH-FLOW states occurs as a normal process in new vessel growth

and is called arteriogenesis (Figure 2).⁶⁻⁸ At one time the processes involved in arteriogenesis were folded into those of angiogenesis, but with increased knowledge of new vessel development the differences in angiogenesis and arteriogenesis became apparent. Angiogenesis is the sprouting of new capillaries, while arteriogenesis is the dilation of preexisting channels by active proliferation and remodeling of the vessel wall. An intriguing difference is that angiogenesis is highly VEGF dependent while arteriogenesis is not VEGF dependent.⁹⁻¹¹ Thus treatment of 1 aspect in neovascularization may not necessarily affect other aspects.

Flow through blood vessels puts various stresses on the vessel. The most important is shear stress, caused by the moving blood over the endothelial cells.^{12,13} Shear stress is directly related to flow and inversely related to the cube of the vessel radius. The pressure required to maintain flow causes circumferential stress on the wall of the vessel. Mechanotransducers in vascular endothelial cells are activated by increased stress. Matrix metalloproteinases are released, integrins activated, and a host of inflammatory cells are recruited to the wall of the vessel. This leads to breakdown and remodeling of the extracellular matrix within the vessel wall and expansion of the vessel. Smooth muscles cells are recruited to the vessel wall, largely through the release of PDGF.

The differing role that VEGF plays in angiogenesis as opposed to arteriogenesis is striking, but another difference, although not as categorical, is the integral involvement of the inflammatory system in arteriogenesis. The innate and adaptive immune systems appear to be needed for arteriogenesis to maximally function. Monocyte depletion in both rabbit and mouse models leads to impaired arteriogenesis, which could be restored by injection of exogenous monocytes. In particular, arteriogenesis appears to be related to M2 macrophages. Genetically CD4-or CD8-deficient mice have impaired arteriogenesis that can be restored by reconstitution with the absent lymphocyte type. Chemokines, tumor necrosis factor- α , TGF α , TGF β , interferon- γ , toll-like receptors 2 and 4, and basic fibroblastic growth factor are involved in arteriogenesis as well.¹⁴ If there is local tissue hypoxia, for instance, coordination would occur between new sprouts of capillaries and the eventual expansion of these capillaries into larger feeding and draining vessels. Feedback mechanisms titrate the amount of increased tissue perfusion vs the reduction in the local tissue hypoxia.

OPTIMAL VASCULAR NETWORKS

LEONARDO DA VINCI MADE THE OBSERVATION IN HIS notebooks¹⁵ that the branches of a tree at every stage of its height, when put together, are equal in thickness to the trunk. In a more modern way of stating this, the radius

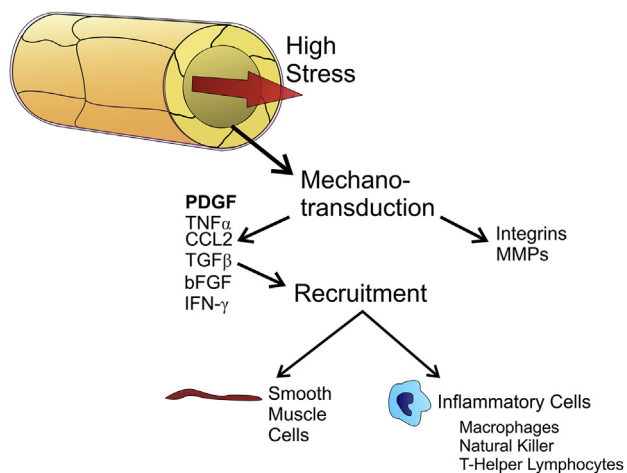


FIGURE 2. Arteriogenesis. Flow through vessels, particularly high flow with its attendant shear stress, stimulates mechanotransducers in vascular endothelial cells. Additional stress, such as stretching along the circumference of the vessel, plays a role also. Activation and release of matrix metalloproteinases (MMPs) and integrins function to break down the basement membrane and proteins within and around the vessel wall. Signaling occurs through the release of many cytokines and chemokines, the most important of which is platelet-derived growth factor (PDGF). These and other factors help in the recruitment of inflammatory cells and also, in some cases, smooth muscle cells. The orchestrated effect of this process leads to rapid structural expansion of the vessel wall. TNF, tumor necrosis factor; CCL2, chemokine (C-C motif) ligand 2; TGF, transforming growth factor; bFGF, basic fibroblastic growth factor; IFN, interferon. These responses are generic through the body and not ocular-specific.

of the parent branch, r_1 , equals the sum of the radii of the daughter branches, r_2 , or $r_1 = r_2 + r_2$. However, from the context of the descriptions as well as the appearance of his drawings it seems that he meant that the cross-sectional area of the parent branch equaled the cross-sectional area of the daughter branches. Thus $r_1^2 = r_2^2 + r_2^2$ has become to be known as da Vinci's law of branching. Note that both daughter branches are shown as r_2 , but the branching does not have to be symmetrical.

About 3 centuries after the death of da Vinci, Jean Léonard Marie Poiseuille was born. He analyzed the flow of fluid in pipes and developed the relationship resistance = $8\eta l / (\pi r^4)$, where η is the viscosity, l is the length, and r is the radius of the pipe. From this we see that small changes in radius have a large effect on flow. However, in a biologic system there is a cost to the organism to make and maintain blood and blood vessels. Charles Murray published a series of papers in the 1926 in which he calculated the optimum diameters of blood vessels and branching that minimized total work on the part of the organism.¹⁶⁻¹⁸ By analyzing the relationship between the cost of a vessel vs the flow through a vessel of any given

diameter, he found the relationship $r_1^3 = r_2^3 + r_2^3$ as an optimum. This relationship is known as Murray's law. Later study showed widespread application of Murray's law to biologic systems. In plants water transport systems follow Murray's law¹⁹ unless they have structural duties, such as in larger tree branches, and then the ratios can approach da Vinci's law.^{20,21} In animals the branching of bronchioles is described by Murray's law, as are blood vessels. However, the exact relationship varies from tissue to tissue. The branching of blood vessels follows a general form of $r_1^x = r_2^x + r_2^x$, where x can range from 2.6 to 3.2. For the retina the value of x is estimated to be 2.85 (Figure 3).²¹

The diameter of successive branches of blood vessels follows the same modified Murray's law and therefore, over the scale of blood vessel sizes, defines a fractal pattern. Of interest is that the segment length of any branch can be summarized as a function of its radius. For the retina the expression is $l = 7.4r^{1.15}$, where l is the length and r is the radius.²² Even the branching angles of vessels can be calculated; as shown by Murray,¹⁸ the angles of branching are related to the relative proportions of the daughter vessel radii.

The theoretically derived values for blood vessels are based on simple goals of minimizing work, but what is the relationship between these parameters and actual vascular circuits? Sherman and associates²³ determined that the majority of branches in a vascular circuit had energy cost functions less than 1% above the Murray minimum and the deviation for entire vascular trees departed from optimal by an average of less than 10%. Although the derivation of optimal flow characteristics has occurred recently over human history, evolutionary derivation of the same features happened much earlier. The efficiency of blood flow in cancer is much lower; Less and associates estimate that energy losses above the Murray optimum for entire trees in mammary carcinoma may be on the order of 40%–100%.²⁴ While the values of the parameters undoubtedly differ by tissue and disease, if CNV grew with the same fractal parameters as do retinal vessels, a representation of the vessels could be generated; Figure 4 shows a fractal "tree" of vessels so derived. The exact format of the vascular tree in life is dependent on tissue needs, but the basic character of vessels growth and patterning shows consistency across many normal tissue types. This consistency seems to break down in local environments where the cytokine levels are presumed to be highly abnormal, such as in tumors.

ABNORMAL VESSEL DEVELOPMENT AND "VASCULAR NORMALIZATION"

FOLKMAN PROPOSED THAT ADMINISTRATION OF ANTIANGIOGENIC DRUGS COULD STARVE TUMORS OF THEIR SOURCE OF OXYGEN

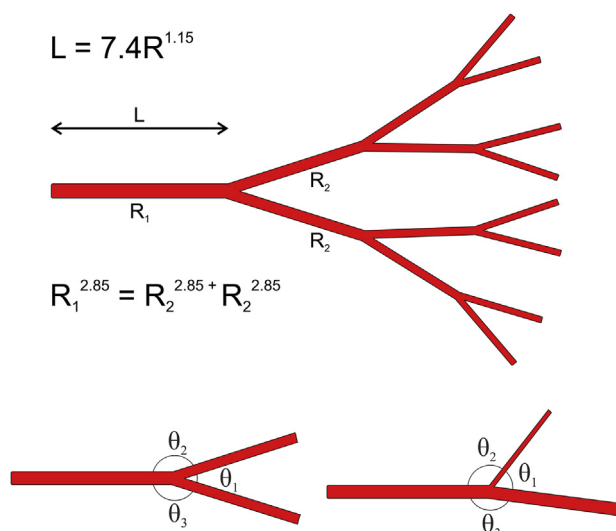


FIGURE 3. Fractal nature of retinal vascular structure. (Top) The branching nearly follows Murray's law, where the sum of cubes of the radii of the daughter vessels equals the cube of the parent vessel. Although the daughter vessels are drawn as symmetrical equal branches, this is for stylistic convenience. The length of a retinal vascular segment is related to the radius of that segment, as per the formula shown.²¹ (Bottom) Murray also calculated how branch angles for various-sized daughter vessel segments can be optimized to minimize work. Symmetrical branching of equal segments (similar to how the common iliac arteries branch from the aorta) is shown at Bottom left, while asymmetrical segments are shown Bottom right. (For the actual equations see reference 17.) Note that only 2 of the angles need to be explicitly stated, but for illustration purposes all 3 are shown. Each branching step follows the general mathematical rules shown in these panels to establish the fractal patterning of retinal vessels.

and nutrition by inhibiting vascular supply.²⁵ Eventually VEGF was discovered and agents designed to bind to VEGF were developed. In clinical use it became apparent that anti-VEGF treatment did not lead to tumor starvation or even prolong survival for many forms of cancer. Instead of an orderly branching network of vessels, newly growing vessels in tumors can appear as bizarre vessels with saccular dilations, shunts, and numerous anastomoses.²⁶ The vessels produced are leaky, and account for the increased hydrostatic pressure seen in tumors. In addition, the aberrant vascular formation does not appear to be able to effectively supply oxygen to the tumor tissue.

In a series of articles,^{27–29} Jain highlighted these features and questioned the mechanisms by which antiangiogenic treatments worked in cancer therapy. The efficacy of antiangiogenic treatment in cancer has been a disappointment, but when given seems to accentuate the effects of ionizing radiation or chemotherapy. Ionizing radiation depends in part on oxygen levels; chemotherapy works only if it is delivered to the growing



FIGURE 4. A fractal vascular tree showing branching approximating the scale in the retina. Note the extensive branching of the vessels shown in red and the large amount of capillaries shown in white. The venous return is not shown.

cancer tissue. Jain hypothesized that the abnormal vascular phenotype in tumors was secondary to excessive angiogenic cytokines³⁰ and that antiangiogenic treatment pruned the more anomalous portions.^{27–29} After antiangiogenic treatment in animal models the remaining vascular network appears more normal, blood flow and oxygen delivery is improved, and the tissue hydrostatic pressure is reduced. Thus the idea of “vascular normalization” was developed. The normalization was proposed to be transient, as the angiogenic cytokines would again induce exuberant proliferation of vascular endothelial cells once the antiangiogenic drugs wane. The idea of vascular normalization was extended to potentially include CNV, with the proposal to use drugs targeting PDGF as a promising combination therapy in AMD.³¹

THE EYE AS A LABORATORY FOR ANTIANGIOGENIC DRUGS

THE IDEA OF VASCULAR NORMALIZATION WAS QUITE INFLUENTIAL, but remains unproven in humans. Repeated biopsy, or even imaging, of tumors to evaluate blood vessel supply is not a routine practice in cancer patients, who are subjected to numerous interventions as part of their normal therapies. On the other hand, repeated ocular imaging of patients treated with antiangiogenic therapy is a standard of care and, depending on the treatment strategy used, can be

performed monthly. The predominant morphology of most treated CNV is fibrovascular pigment epithelial detachments. Fluorescein angiography is poor at visualizing the interior of fibrovascular PEDs, but has utility in evaluating leakage from them. Indocyanine green angiography offers better visualization of the vessels within the PED because the excitation and resultant fluorescence is in the near-infrared region, which penetrates through pigmented layers better than do the shorter wavelengths used by fluorescein. Even so, the multiple layers of vessels in the eye are all imaged simultaneously; the images often have low contrast; and, as with fluorescein, there is a risk, albeit low, from the dye injection. Nondye angiography based on optical coherence tomography (OCT) is capable of imaging vessels based on flow and consequently does not require dye injections.³² Similar to other forms of OCT imaging, structures visible in OCT angiography can be separated by segmenting the anatomy based on anatomic features and the vessels are not obscured by staining or leakage. As such, vascular layers can be isolated and studied in detail. Analyzing the vascular structure of treated CNV would provide information concerning the response to treatment, and may provide clues as to the vascular structure in tumors treated with periodic anti-VEGF medications.

METHODS

THIS RETROSPECTIVE STUDY WAS APPROVED BY THE Western Institutional Review Board and complied with the Health Insurance Portability and Accountability Act of 1996. Eyes in this study had preliminary OCT evaluation with the Heidelberg Spectralis (Heidelberg Engineering, Mountain View, California, USA) as part of the normal evaluation workflow of patients with CNV. From these scans the greatest linear dimensions of the lesions were measured, by evaluating the infrared scanning laser ophthalmoscopic images and the successive OCT scans within the volume scan.

• **OPTICAL COHERENCE TOMOGRAPHY ANGIOGRAPHY:** The instrument used for OCT angiography (OCTA) images is based on the Optovue RTVue XR Avanti (Optovue, Inc, Fremont, California, USA) to obtain amplitude decorrelation angiography images. This instrument has an A-scan rate of 70 000 scans per second, using a light source centered on 840 nm and a bandwidth of 45 nm. Each OCTA volume contains 304×304 A-scans with 2 consecutive B-scans captured at each fixed position before proceeding to the next sampling location. The scan area was 3×3 mm. Split-spectrum amplitude-decorrelation angiography was used to extract the OCT angiography information.³³ Each OCTA volume is acquired in 3 seconds and 2 orthogonal OCTA volumes were acquired in order to perform motion correction to minimize motion artifacts arising from microsaccades and fixation changes.³⁴ Angiography information

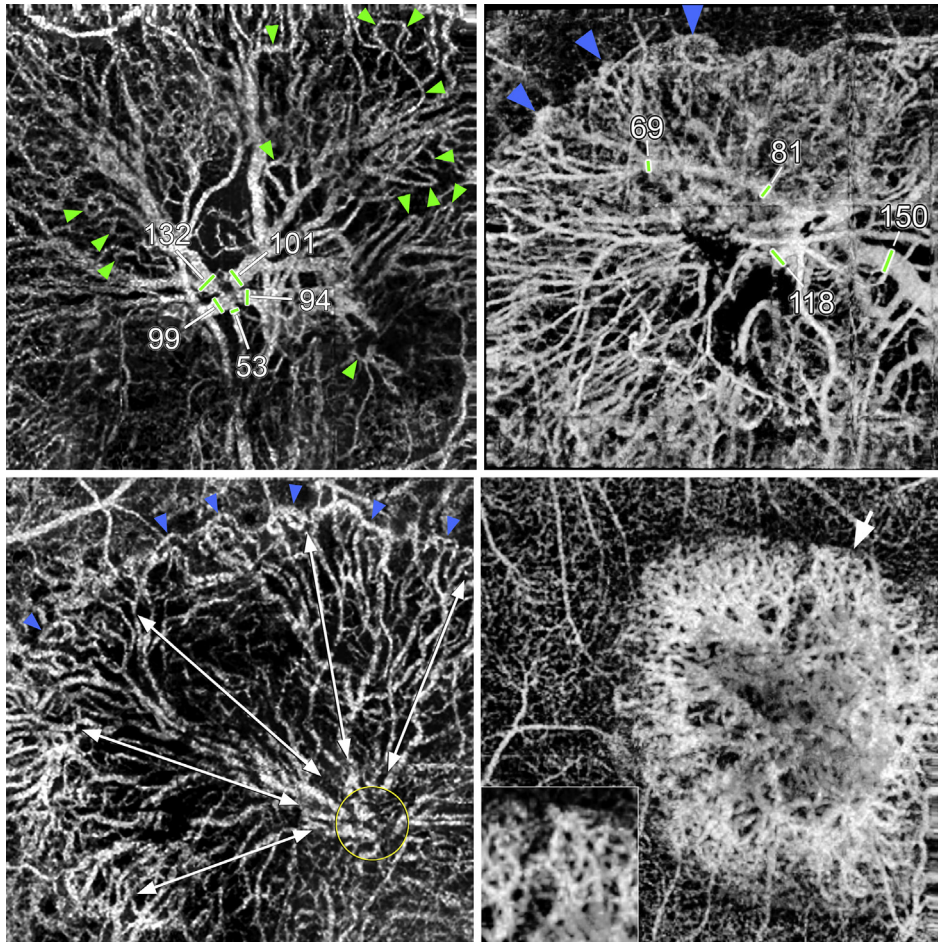


FIGURE 5. Optical coherence tomography angiography of treated choroidal neovascularization. (Top left) The sizes of the main trunk vessels (in μm) are shown. The lesion size is approximately $4700 \mu\text{m}$ in greatest linear dimension (data not shown); however, the trunk vessels approximate the diameter of the major arcade vessels. Note the multiple loops and shunts present (green arrowheads). The pattern of these vessels does not follow the generic branching structure of retinal vessels as shown in Figure 3. The visual acuity is 20/30 and the eye had 49 anti-vascular endothelial growth factor (VEGF) injections. (Top right) This neovascular lesion is approximately $4000 \mu\text{m}$ in greatest linear dimension. Note the large diameter of the trunk vessels (shown in μm) and the terminal loops of the vessels (blue arrowheads) that appear to have anastomotic connections at the outer border of the neovascularization. The visual acuity was 20/40 and the eye had 54 intravitreal anti-VEGF injections. (Bottom left) The yellow circle encompasses the trunk vessels of the lesion. Note the long extent of the vessels as they reach the edge of the lesion (white double arrows) and the relative lack of branching. Shunt vessels are visible within the lesion. At the periphery there appears to be a clearly defined anastomotic connection around the border (blue arrowheads). The visual acuity was 20/80 and the eye had 29 intravitreal anti-VEGF injections. (Bottom right) This lesion has multiple trunk vessels measuring $100 \mu\text{m}$ or greater. The vessels course outward toward the edge of the lesion, which is $2300 \mu\text{m}$ in greatest linear dimension. The outer portion of the lesion was composed of many medium-sized vessels, approximately $40 \mu\text{m}$ in diameter, that formed interconnections with each other. The dense network of these vessels suggested a latticework. An enlargement of the area highlighted by the white arrow is shown as an inset. The visual acuity was 20/40 and the patient had 42 intravitreal injections.

displayed is the average of the decorrelation values when viewed perpendicularly through the thickness being evaluated. This methodology does not use phase information from the OCT signal.

- **SEGMENTATION OF THE OPTICAL COHERENCE TOMOGRAPHY ANGIOGRAPHIC IMAGE:** To evaluate the blood vessels within the fibrovascular PED, the layers were segmented by fitting a curve to the region directly under the Bruch membrane. A similar curve was offset through

the thickness of the tissue being evaluated and the volume of tissue between the 2 planes was evaluated. The thickness can be offset from above or below the starting level to obtain slices of tissue at any arbitrary location. Light entering a retinal vessel can strike a formed blood element, which can lead to reflection, adsorption, or refraction. The temporal variation in the reflected light forms the basis that decorrelation methods use in image creation. Moment-to-moment changes in reflected light caused by a moving blood element decreases local correlation in a

region and decorrelation is interpreted to represent flow. The problem with this technique is that temporally changing patterns of light are interpreted as flow even if the structures themselves are not moving. Light passing through blood vessels can be reflected from deeper structures such as the RPE. This reflected light is not constant, as it varies over time in its passage through the overlying retinal vessels. Since this light varies with time, an image of the retinal blood vessels can be artifactually obtained by segmenting at or near the level of the RPE. This means sections through the tissue that include the RPE may show images of the retinal vessels even though the sections do not specifically include the retinal vessels.

• **TREATED FIBROVASCULAR PIGMENT EPITHELIAL DETACHMENTS:** Patients with fibrovascular pigment epithelial detachments were imaged in this study. Acute PEDs related to choroidal neovascularization secondary to AMD often have varying amounts of blood and fluid; the current segmentation scheme used cannot provide reliable or accurate results in the face of large amounts of these materials. In addition, blood masks underlying structures. Treated patients have a much lower proportion of these components with typically better visual acuity, and therefore they are more readily imaged. Fibrovascular pigment epithelial detachments were defined as dome-shaped elevations of the RPE by fibrovascular material. To be considered an elevation, the outer boundary of the RPE must have exceeded the height of the adjacent inner boundary of RPE in regions that were not affected. OCT angiography using the technique employed in this study requires patients to hold their eye steady for 3–4 seconds, and motion control software cannot compensate for information lost during movement. Patients with very poor acuity cannot maintain accurate fixation and therefore were not candidates. Visualization of vessels is difficult with lower signal strength levels. Therefore patients with a visual acuity of 20/100 or less and those with a signal strength of 55 or less were not included in this study. This retrospective study was of consecutive patients meeting these requirements. To help visualize the vessels in the fibrovascular PED, some of the eyes had consecutive sections made at 9 μm , which were then exported from the Optovue program. These were then imported into the program Medical Image Processing, Analysis, and Visualization (US National Institutes of Health, Bethesda, Maryland, USA) for volume rendering.

RESULTS

THERE WERE 17 EYES OF 14 PATIENTS EVALUATED IN THIS study (8 men and 6 women), and the mean age of the patients was 78.4 (standard deviation \pm 9.3) years. The patients had a mean visual acuity of 0.326 logMAR

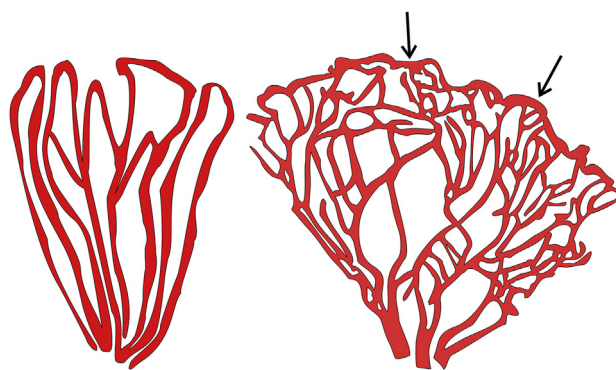


FIGURE 6. To compensate for the lack of good descriptors for vessel shape and branching, a stylized drawing of the vessels in a choroidal neovascular lesion given periodic anti-VEGF treatments was made. (Left) Some lesions had the outer terminus composed of vascular loops, while (Right) other lesions had an anastomotic vessel bounding the outer border of the vascular lesion (arrows). Contrast these diagrammatic representations with the fractal branching seen in Figure 3.

(20/42 Snellen equivalent, interquartile logMAR range 0.239–0.438) and received a mean of 47 (\pm 21) intravitreal anti-VEGF injections. The mean greatest linear dimension was 3600 (\pm 1480) μm . The vascular networks seen in the patients of this study shared similar characteristics (Figure 5). All patients demonstrated prominent vascular loops and anastomotic connections. The main trunk vessels, also called “feeder” vessels, were large in diameter, given the relatively small lesion sizes. The vessels in the neovascularization did not appear to branch as frequently as would be expected if they followed the generic fractal pattern of the retinal vessels, and the diameter of the vessels remained relatively large even to the periphery of the neovascular lesions (Figure 5). At the outer border a circumferential anastomotic border was seen in 5 eyes (31.3%). The remaining lesions had loops of larger vessels seen at the outer periphery. One eye had a large lesion in which the full extent of the periphery could not be evaluated; this lesion was 7400 μm in greatest linear dimension. In all eyes there was a paucity of capillaries visualized. Two representative drawings were made illustrating the vascular patterns present in these eyes (Figure 6).

DISCUSSION

THE CHOROIDAL NEOVASCULARIZATION EXAMINED IN THIS descriptive study shared common vascular features when examined by OCT angiography. The trunk vessels were large in diameter, given the relatively small lesion sizes; the vessels within the lesions showed limited branching as they coursed to the peripheral portions of the lesion; and there were prominent anastomotic connections

between large-diameter vessels. The vascular diameter did not appear to follow the fractal branching arrangement expected if they were to follow the same pattern as retinal vessels. In addition, a variable amount of peripheral anastomosis existed at the border of many lesions. These observations do not preclude the possibility of capillaries being present, but not visualized, within the lesions. However, the salient characteristics were the large diameter and prominent anastomoses of the vessels in treated CNV.

In the early process of growth of the CNV lesion the histology resembles that of granulation tissue.³⁵ Untreated CNV grows in size, and is accompanied by bleeding, leakage, and exudation. For untreated eyes this process resolves with the formation of a macular scar, much the same as transition from granulation tissue to scar in other areas of the body. While there are many theories of why CNV occurs and grows in the macula, the resolution of the process coincident with the destruction of the macula and the disruption of underlying layers like the RPE suggests that the process is efficient at resolving the stimulus for its own formation. Treatment with antiangiogenic agents seeks to blunt or halt the invasion of blood vessels and to reduce the exudative manifestations from the vessels. The anti-VEGF treatment does not address the stimulus for the process. Reducing VEGF halts a significant and necessary step, the sprouting of new capillaries, and also reduces VEGF-mediated vascular leakage.

It appears possible to explain the observed vascular changes by using known features of vascular physiology. With administration of anti-VEGF medications the level of free VEGF drops precipitously, and newly growing vascular sprouts regress (Figure 7 shows this theoretical construct). Vessels with adequate pericyte coverage do not, as the pericytes supply VEGF locally to their associated vascular endothelial cells. The flow through a network is a function of the pressure gradient and the vascular resistance. Closing many newly formed channels, even if small in radius, would increase the vascular resistance for the entire vascular circuit. The remaining patent channels would have a higher pressure differential and thus a higher flow. Increased flow through the remaining channels is the stimulus for arteriogenesis, with its attendant effect of increasing vessel size. As the anti-VEGF medication wanes the levels of unbound VEGF rise, leading to a resumption of capillary sprouting. The capillaries grow out of the vessels that remain, the formerly pruned larger branches. Increased flow can cause these branches to expand in size, again owing to arteriogenesis. Repeated anti-VEGF treatment prunes back the newly growing vessels, to begin the cycle again. Thus the vessel ingrowth is faced with a continuous stimulus for expansion punctuated by periodic inhibition of 1 aspect of the proliferation, namely angiogenesis. The balance between angiogenesis and arteriogenesis as mandated by stimulus for growth is disturbed, with arteriogenesis not being inhibited.

An analogy can be made comparing periodic treatment with anti-VEGF agents to the steps used to produce a

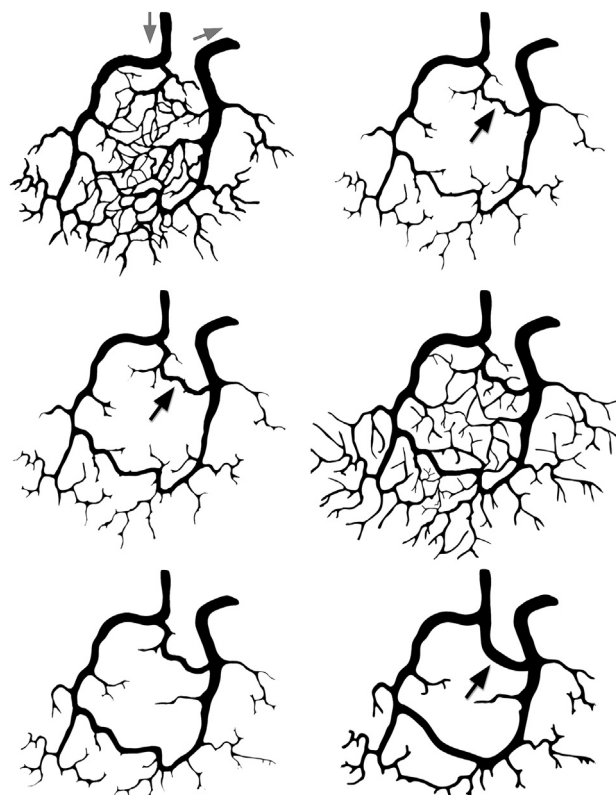


FIGURE 7. Proposed stages of vascular change with periodic anti-vascular endothelial growth factor (VEGF) treatment. (Top left) High levels of cytokines such as VEGF lead to exuberant vascular proliferation. The blood flow into and out of the vascular bed is shown by the gray arrows. (Top right) After anti-VEGF injection, the levels of free VEGF drop precipitously and there is corresponding regression of the newly growing vessels, particularly those with poor pericyte coverage. Some tubes that have pericyte coverage remain (arrow). (Middle left) With increased flow through the remaining vessels, arteriogenesis leads to an increase in vascular diameter (arrow). (Middle right) As the anti-VEGF drug wanes, the levels of free VEGF increase and lead to regrowth of the vascular sprouts. (Bottom left) Pruning of the sprouts concomitant with the administration of anti-VEGF medication leaves the now larger vascular tubes. (Bottom right) After numerous iterations the formerly capillary-sized connections between the efferent and afferent vessels have enlarged to shunt vessels (1 being highlighted by the arrow). The large size of the anastomotic connections means the pressure differential between the efferent and afferent sides of the vascular tree is decreased. These responses would be generic and not ocular-specific.

bonsai tree. There are 2 principal ways trees grow: the tips of branches grow and branch through the proliferation of apical meristem tissue, and the branches can increase in diameter through the production of more tissue (xylem and phloem) by the vascular cambium. A bonsai tree is created over years of time by repeatedly pruning back the buds and newly growing branches of the tree.³⁶ In the interim the trunk and larger branches continue to grow larger in

diameter, to produce small trees with large trunks. The growth from the apical meristems is analogous to the growth and branching of vascular sprouts, angiogenesis, while the expansion of the trunk and large branches is analogous to arteriogenesis. The analogy serves as a teaching tool to illustrate how the iterative nature of modifying the normal progression of growth and pruning can produce an altered phenotype.

There are possible treatment implications that may be related to the changed phenotype. In an ordinary vascular bed the progressively decreasing branch diameters of the arterial system help diminish the blood pressure at each stage, both by passive frictional effects and by active autoregulation. As such, the transmural pressure at the terminal capillaries has the potential to be exquisitely controlled. The vessels present in eyes having received recurrent anti-VEGF treatment are large and display numerous connections between the efferent and afferent vessels of the CNV. The large channel size suggests that the flow should be relatively unimpeded and thus the pressure differential should be relatively low. Therefore any growing sprouts from these vessels would be subject to relatively high transmural pressure. If this is the case, a disproportionate amount of leakage could occur. Small amounts of capillary growth would be associated with a disproportionately large amount of leakage, thus necessitating frequent treatment. In addition, this possibility may help explain the higher incidence of hemorrhage in eyes with a decreased dosing schedule of ranibizumab.³⁷

It is possible that the vascular response of new vessel growth in other conditions to repeated periodic anti-VEGF injections could mirror those found in the patients of the present study. Inspection of a small number of eyes treated with multiple bevacizumab injections for neovascularization secondary to retinopathy of prematurity has shown the presence of multiple peripheral arteriovenous shunts at the boundaries of previous areas of neovascularization. An example is shown in Figure 8. Additional research in the response of neovascularization in retinopathy of prematurity seems indicated. Retinal neovascularization in diabetic retinopathy appears to show pronounced regression following anti-VEGF injection, implying that the recruitment of pericytes may be different in this situation. Tumor resistance to anti-VEGF therapies, unfortunately, is common, and even if the tumor type is sensitive the benefit is temporary.³⁸⁻⁴⁰ While there may be many mechanisms by which tumors gain anti-VEGF resistance, one may be the dilation of vascular channels related to periodic administration of anti-VEGF agents similar to what is seen in choroidal neovascularization. The architecture of the vessels could shift toward the resistance to VEGF withdrawal by continued arteriogenesis.

The present study has numerous limitations. The current series of patients used a first-generation OCT angiography device that was difficult for some patients because of fixation and the need to avoid eye movement during

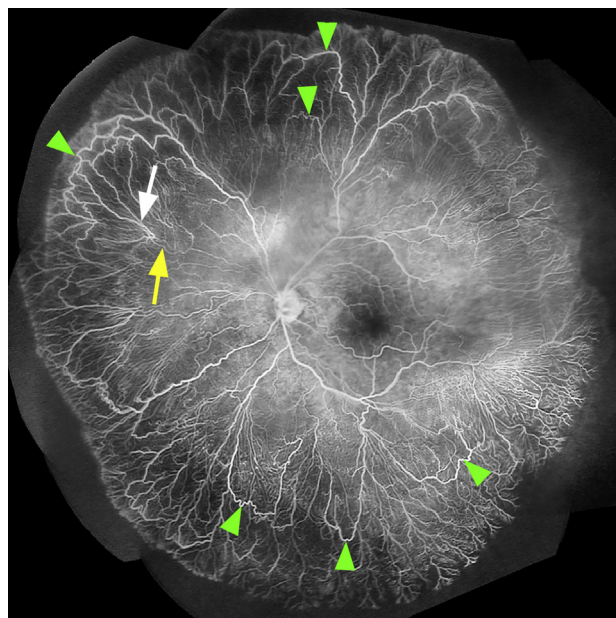


FIGURE 8. Fluorescein angiogram of an eye with retinopathy of prematurity after several treatments with bevacizumab. In retinopathy of prematurity there can be pathologic proliferation of neovascularization out of the plane of the retina. Injection of bevacizumab causes regression of the new vessels followed by continuing physiologic vascularization of the more peripheral retina. After pruning of the neovascularization by bevacizumab, remaining vascular channels could undergo the effects of arteriogenesis according to the hypothesis generated in this paper, thus explaining the anastomotic connections at previous tide-marks of neovascularization. The retinal vascular shunts (green arrowheads) are arranged in tiers. Note the relatively large size of some of the vessels in the periphery (white arrow) as compared with the arcade vessels near the disc, or even the proximal vessels (yellow arrow), thus violating the vascular patterning shown in Figure 3. (Fluorescein angiogram image courtesy of Audina Berrocal.)

the scan process. The sensitivity fall-off with depth and the problems of image segmentation of abnormal tissue makes imaging untreated lesions difficult. Therefore the untreated CNV is difficult to adequately image at present. This ability may change in the future. The morphology in the untreated state may change after the first treatment or so to emulate the transient normalization seen in tumor vessels after antiangiogenic treatment. Given the efficacy of modern treatments and the poor outcome for untreated eyes, the OCT angiography of the natural history of CNV is not likely to be known. Consequently the present findings of treated CNV from this study exist in isolation. However, because the proportion of treated patients with useful vision will continue to increase over time secondary to effective treatment, investigation of lesion vascularity may prove valuable in both understanding and managing neovascular AMD. There is likely a life cycle to the neovascular process. It is possible that with

atrophy there is loss of the tissue eliciting the growth of CNV and in that situation there would be less need for anti-VEGF injections. There have been large research efforts devoted to studying the potential risk factors for AMD, the genetic associations, aspects of cell physiology, tissue interactions, and imaging characteristics of the eye as it progresses toward late AMD, but there is a paucity of information available regarding the vessel characteristics of treated CNV. OCT angiography appears to be an imaging modality that can be exploited for this purpose, particularly in light of expected technical improvements expected to occur over time. The ability to image based on blood flow provides an opportunity to improve our understanding of exudative lesions in late AMD and may offer methods of gauging treatment effect.

Strategies for the economical management of flow in vessels has been characterized by humans over the last century or so, but has been honed over hundreds of millions of years of evolution. Growth, selection, and pruning of vessels are tactics used in managing vascular networks in health and

disease. The normal transition from granulation tissue to scar illustrates how vascular pruning is part of the life cycle of tissue maturation. Current therapy of CNV for AMD relies on periodic pruning of newly growing vessels by pharmacologic intervention in the context of chronic stimulus for their growth. While this approach blunts the progression of some disease processes, the same strategy appears to alter the morphology of the remaining vascular bed. The induced changes are likely to have therapeutic consequences. The eye is a readily accessible organ where blood vessels can easily be seen and evaluated by multiple test modalities. Cytokine levels can be measured in ocular fluids, although the exact relationship to tissue levels has not been quantified. Injection into the vitreous of anti-VEGF agents is performed in the treatment of a variety of important ocular diseases, and these injections may be given repeatedly over years of therapy. Thus the eye is a laboratory for studying the effects of VEGF blockade. Learning about the effects in 1 disease may carry over to other ocular diseases or to systemic conditions such as cancer.

THE AUTHOR HAS COMPLETED AND SUBMITTED THE ICMJE FORM FOR DISCLOSURE OF POTENTIAL CONFLICTS OF INTEREST. Financial Disclosure: Richard F. Spaide receives consultant and royalty payments from Topcon Medical Systems, Oakland, New Jersey. Funding/Support: Supported in part by the Macula Foundation, New York, New York. The support involved no input to the content or wording of the article. The author attests that he meets the current ICMJE requirements to qualify as author.

Fluorescein angiogram of treated retinopathy of prematurity kindly supplied by Audina Berrocal, MD, Bascom Palmer Eye Institute, Miami, Florida. Christine Curcio, PhD, University of Alabama, Birmingham, Alabama, supplied helpful comments in a review of this manuscript.

REFERENCES

1. Spaide RF. Enhanced depth imaging optical coherence tomography of retinal pigment epithelial detachment in age-related macular degeneration. *Am J Ophthalmol* 2009; 147(4):644–652.
2. Comparison of Age-related Macular Degeneration Treatments Trials (CATT) Research Group Martin DF, Maguire MG, et al. Ranibizumab and bevacizumab for treatment of neovascular age-related macular degeneration: two-year results. *Ophthalmology* 2012;119(7):1388–1398.
3. Adams RH, Alitalo K. Molecular regulation of angiogenesis and lymphangiogenesis. *Nat Rev Mol Cell Biol* 2007;8(6): 464–478.
4. Weis SM, Cheresh DA. Tumor angiogenesis: molecular pathways and therapeutic targets. *Nat Med* 2011;17(11): 1359–1370.
5. Carmeliet P. Mechanisms of angiogenesis and arteriogenesis. *Nat Med* 2000;6(4):389–395.
6. Potente M, Gerhardt H, Carmeliet P. Basic and therapeutic aspects of angiogenesis. *Cell* 2011;146(6): 873–887.
7. Scholz D, Cai WJ, Schaper W. Arteriogenesis, a new concept of vascular adaptation in occlusive disease. *Angiogenesis* 2001; 4(4):247–257.
8. Chachisvilis M, Zhang YL, Frangos JA. G protein-coupled receptors sense fluid shear stress in endothelial cells. *Proc Natl Acad Sci U S A* 2006;103(42):15463–15468.
9. Deindl E, Buschmann I, Hofer IE, et al. Role of ischemia and of hypoxia-inducible genes in arteriogenesis after femoral artery occlusion in the rabbit. *Circ Res* 2001; 89(9):779–786.
10. Schierling W, Troidl K, Troidl C, Schmitz-Rixen T, Schaper W, Eitenmüller IK. The role of angiogenic growth factors in arteriogenesis. *J Vasc Res* 2009;46(4):365–374.
11. Wu S, Wu X, Zhu W, Cai WJ, Schaper J, Schaper W. Immunohistochemical study of the growth factors, aFGF, bFGF, PDGF-AB, VEGF-A and its receptor (Flk-1) during arteriogenesis. *Mol Cell Biochem* 2010; 343(1-2):223–229.
12. Pipp F, Boehm S, Cai WJ, et al. Elevated fluid shear stress enhances postocclusive collateral artery growth and gene expression in the pig hind limb. *Arterioscler Thromb Vasc Biol* 2004;24(9):1664–1668.
13. Tzima E, Irani-Tehrani M, Kiosses WB, et al. A mechanosensory complex that mediates the endothelial cell response to fluid shear stress. *Nature* 2005;437(7057): 426–431.
14. la Sala A, Pontecorvo L, Agresta A, Rosano G, Stabile E. Regulation of collateral blood vessel development by the innate and adaptive immune system. *Trends Mol Med* 2012; 18(8):494–501.
15. Da Vinci L, Ukray M (illustrator), Richter JP (translator). *The Notebooks of Leonardo Da Vinci: Complete & Illustrated*. Las Vegas, Nevada: CreateSpace Independent Publishing Platform; 2014.

16. Murray CD. The physiological principle of minimum work: I. The vascular system and the cost of blood volume. *Proc Natl Acad Sci U S A* 1926;12(3):207–214.
17. Murray CD. The physiological principle of minimum work: II. Oxygen exchange in capillaries. *Proc Natl Acad Sci U S A* 1926;12(5):299–304.
18. Murray CD. The physiological principle of minimum work applied to the angle of branching of arteries. *J Gen Physiol* 1926;9(6):835–841.
19. McCulloh KA, Sperry JS, Adler FR. Water transport in plants obeys Murray's law. *Nature* 2003;421(6926):939–942.
20. Eloy C. Leonardo's rule, self-similarity, and wind-induced stresses in trees. *Phys Rev Lett* 2011;107(25):258101.
21. Minamino R, Tateno M. Tree branching: Leonardo da Vinci's rule versus biomechanical models. *PLoS One* 2014; 9(4):e93535.
22. Takahashi T. *Microcirculation in Fractal Branching Networks*. Tokyo: Springer Japan; 2014.
23. Sherman TF, Popel AS, Koller A, Johnson PC. The cost of departure from optimal radii in microvascular networks. *J Theor Biol* 1989;136(3):245–265.
24. Less JR, Skalak TC, Sevick EM, Jain RK. Microvascular architecture in a mammary carcinoma: branching patterns and vessel dimensions. *Cancer Res* 1991;51(1): 265–273.
25. Folkman J. Tumor angiogenesis: therapeutic implications. *N Engl J Med* 1971;285(21):1182–1186.
26. Nagy JA, Chang SH, Dvorak AM, Dvorak HF. Why are tumour blood vessels abnormal and why is it important to know? *Br J Cancer* 2009;100(6):865–869.
27. Jain RK. Normalizing tumor vasculature with anti-angiogenic therapy: a new paradigm for combination therapy. *Nat Med* 2001;7(9):987–989.
28. Jain RK. Normalization of tumor vasculature: an emerging concept in antiangiogenic therapy. *Science* 2005;307(5706): 58–62.
29. Carmeliet P, Jain RK. Principles and mechanisms of vessel normalization for cancer and other angiogenic diseases. *Nat Rev Drug Discov* 2011;10(6):417–427.
30. Ozawa CR, Banfi A, Glazer NL, et al. Microenvironmental VEGF concentration, not total dose, determines a threshold between normal and aberrant angiogenesis. *J Clin Invest* 2004;113:516–527.
31. Spaide RF. Rationale for combination therapies for choroidal neovascularization. *Am J Ophthalmol* 2006; 141(1):149–156.
32. Spaide RF, Klancnik JM Jr, Cooney MJ. Retinal vascular layers imaged by fluorescein angiography and optical coherence tomography angiography. *JAMA Ophthalmol* 2015; 133(1):45–50.
33. Jia Y, Tan O, Tokayer J, et al. Split-spectrum amplitude-decorrelation angiography with optical coherence tomography. *Opt Express* 2012;20(4):4710–4725.
34. Kraus M, Liu J, Schottenhamml J, et al. Quantitative 3D-OCT motion correction with tilt and illumination correction, robust similarity measure and regularization. *Biomed Opt Express* 2014;5(8):2591–2613.
35. Grossniklaus HE, Miskala PH, Green WR, et al. Histopathologic and ultrastructural features of surgically excised subfoveal choroidal neovascular lesions: submacular surgery trials report no. 7. *Arch Ophthalmol* 2005;123(7): 914–921.
36. Chan P. *Bonsai: The Art of Growing and Keeping Miniature Trees*. New York: Skyhorse Publishing; 2014.
37. Barbazetto I, Saroj N, Shapiro H, Wong P, Freund KB. Dosing regimen and the frequency of macular hemorrhages in neovascular age-related macular degeneration treated with ranibizumab. *Retina* 2010;30(9): 1376–1385.
38. Ellis LM, Hicklin DJ. Pathways mediating resistance to vascular endothelial growth factor-targeted therapy. *Clin Cancer Res* 2008;14(20):6371–6375.
39. Tie J, Desai J. Antiangiogenic therapies targeting the vascular endothelial growth factor signaling system. *Crit Rev Oncog* 2012;17(1):51–67.
40. Abdullah SE, Perez-Soler R. Mechanisms of resistance to vascular endothelial growth factor blockade. *Cancer* 2012; 118(14):3455–3467.